IEEE Photonics Journal
An IEEE Photonics Society Publication

Open Access

Experimental Study of Reconfigurable Visible Light Communications Based on Holographic Spot Array Generations

Volume 10, Number 2, April 2018

Hsi-Hsir Chou
Cheng-Yu Tsai
Chia-Lun Chen

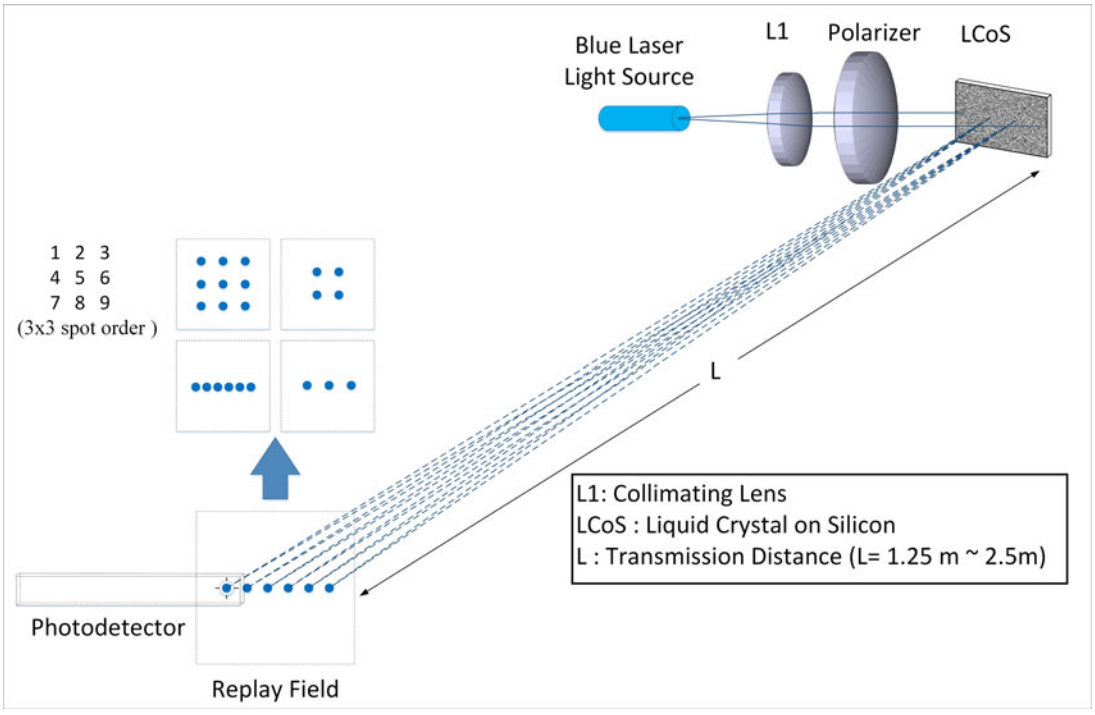

DOI: 10.1109/JPHOT.2018.2817124
1943-0655 © 2018 IEEE

IEEE photonics SOCIETY

IEEE

Experimental Study of Reconfigurable Visible Light Communications Based on Holographic Spot Array Generations

Hsi-Hsir Chou [1,2] **Cheng-Yu Tsai** [1] **and Chia-Lun Chen** [1]

[1]Department of Electronic and Computer Engineering, National Taiwan University of Science and Technology, Taipei 106, Taiwan
[2]Department of Engineering, University of Cambridge, Cambridge CB3 0FA, U.K.

DOI:10.1109/JPHOT.2018.2817124

Manuscript received February 16, 2018; revised March 13, 2018; accepted March 15, 2018. Date of publication March 20, 2018; date of current version April 9, 2018. This work was supported in part by the Ministry of Science and Technology (MOST), Taiwan (MOST 106-2221-E-011-011 and MOST 106-2911-I-011-509) and The Royal Society of Edinburgh (RSE), U.K. (REF_57224). Corresponding author: Hsi-Hsir Chou (e-mail: hsi-hsir.chou@trinity.cantab.net).

Abstract: An experimental study of a reconfigurable visible light communication (VLC) system, using liquid crystal on silicon-based spatial light modulator, which dynamically offers multicast transmission, for indoor optical wireless communication configuration is presented and experimentally demonstrated. The multicast transmission of the system using holographic spot array generation was achieved through an efficient design of near-field computer generated hologram based on Gerchberg–Saxton (GS) algorithm. The system transmission performance, limited by the spot power nonuniformity, was improved through an optimization of GS algorithm, and the results shown that a significant improvement over 11% has been achieved either in a one-dimensional or two-dimensional spot array generations at a transmission distance of 1.25–2.5 m. This paper provides an efficient approach for the direct implementation of a reconfigurable VLC system based on multisport configuration.

Index Terms: Free-space optical communication, spatial light modulators, computer holography.

1. Introduction

With the increasing bandwidth requirement from home multimedia services such as online game and video on demands, Next-Generation Passive Optical Network Stage 2 (NG-PON2) [1] has been proposed to deliver a high-speed data transmission rate over 10 Gbps and above for consumer use in home area networks (HANs). However, the bottleneck problem of consumer use from accessing *Internet* service directly through a high-speed data transmission approach in HANs remain exists due to the difficulties in using and installing optical fibers arbitrary. Although wireless access technologies such as Wi-Fi and WiMAX based on the use of radio frequencies (RF) at microwave range have become a popular access approach in the modern world, a high-speed data transmission service delivered from NG-PON2 cannot be well transferred for consumer use efficiently due to the limited modulation bandwidth of microwave frequencies. Optical wireless solutions based on free-space transmission medium, are emergence as an alternative solution to RF communications [2] for NG-PON2 extension to indoor wireless access due to its variety of advantages such as unregulated free optical spectrum with a higher modulation bandwidth and the immunity of electromagnetic interference.

TABLE 1
LD-Based VLC System Technology

VLC link configuration	Modulation scheme	Link speed limit (BER = 10^{-3})	System capacity	References
Fixed point-to-point (P2P)	Baseband (NRZ_OOK)	4 Gbps (modulation speed of LD)	4 Gbps (modulation speed of LD)	[12]
Fixed point-to-point (P2P)	Multicarrier (64-QAM OFDM)	9 Gbps (modulation speed of LD)	9 Gbps (modulation speed of LD)	[13]
Dynamically point-to-multipoint (P2M)	Baseband / Multicarrier	The lowest transmission rate of the port (spot)	Increase with the number of spots generated	N/A

In the recent technology development of indoor optical wireless communications (OWC), technical solutions based on both direct line-of-sight (LOS) and diffused beam system have been well studied [2], [3] but each has the disadvantages and limitations. Although diffused system is expected to provide a well mobility support for indoor consumer use and several approaches have been proposed to improve its performance which includes adaptive power, angle distribution techniques [4] as well as angle diversity receiver [5], the experimental results demonstrated recently [6] have shown that only limited performance can be improved due to the poor power efficiency and multipath dispersions still creating a severe inter-symbol interference (ISI) and pulse spreading [4], [5]. Although the disadvantages of multipath dispersion and power consumption can be compensated by using LOS solution, alignment difficulty, immobility support for terminal users and transmission interruptions from physical shadowing have made the solution impractical for real application. Several hybrid approaches based on the use of beam steering element such as Microelectromechanical Systems (MEMS) and liquid crystal on silicon (LCoS) device with limited mobility support by avoiding the disadvantages of direct LOS and diffused beam system solutions have been proposed [7], [8] but were all based on a point-to-point (P2P) communication link in which providing point-to-multipoint (P2M) communication links have not yet investigated.

Although the concept of multisport diffusing configuration based on holographic spot array generation was proposed to combine the benefits and to compensative the shortages of a direct LOS or a diffusing configuration for optical wireless access [9], the research works that have been done or are ongoing were all based on computer simulation approaches, and none has been experimentally demonstrated to date [10], [11]. Moreover, the practical challenge on the implementation of a reconfigurable visible light communication (VLC) system based on multispot diffusing configuration through holographic spot array generation is that the nonuniformity of spot array power intensities will limit the system transmission performance. Ideally, the power intensity of the multiple spots should be kept as uniform as possible in order to ensure a more uniform signal power distribution but it is still an objective that is pursuing.

Although the recent experimental researches on VLC technology using laser diode (LD) as the light source have reported that several Gbps data rate can be achieved [12], [13], from our comparisons as shown in Table 1, they were all based on a fixed p2p link configuration. More importantly, their system capacities were also limited to the modulation speed of the light source either when baseband modulation schemes (i.e., NRZ-OOK) or multicarrier modulation schemes (i.e., OFDM) were used. However, when the VLC system are configured in a P2M communication scenario, the system capacity will be dramatically improved while more spots are generated simultaneously for multiuser communications. In this paper, to the best of our knowledge, this is the first time that an experimental VLC system based on holographic spot array generation that has implemented, is presented and demonstrated. In distinguish with previous P2P OWC research based on

beam steering technique, the system use an LCoS-based spatial light modulator (SLM) through an efficient design of near-field (Fresnel approximation [14]) computer-generated holograms (CGHs) based on an optimized gerchberg-saxton (GS) algorithm to dynamically generate multispot either in a one-dimension or two-dimension configurations, potentially for multiuser communications. The system transmission performance for the proof of concept was evaluated at a transmission distance of 1.25 m$\sim$2.5 m. The measurement results in terms of spot power uniformity and data transmission rate shown that a significant performance improvement has achieved either in a one-dimension or two-dimension spot array generations. This research work will provide an efficient approach for the direct implementation of a reconfigurable VLC system based on multisport configuration.

2. Design of Holographic Spot Array Generation Based on LCoS SLM

There are several optical approaches and techniques can be utilized to serve as a spot array generator for multisport diffusing configuration such as Fresnel plane array generator, Image-plane array generator and Fourier plane array generator [15]. Although Image plane array generator are energy efficient, their major drawbacks however are that any inhomogeneity of the incident beam will be transferred to the targeted spots. In the technique of Fresnel plane array generator such as using Talbot imaging, all of the illumination is not easy to be completely directed into the targeted spots [15], [16]. However, both of these two approaches are all not able to generate spot array rapidly and efficiently. Therefore they are not well suitable for dynamically multispot configuration in a reconfigurable VLC system.

In the technique of "Fourier plane array generator", spot arrays with high-contrast are produced when a diffractive grating is Fourier transformed. The profile of spot arrays is transformed from the Gaussian illumination profile. A period of the grating pattern determines the envelope function across these spot arrays. The homogeneity is thus determined by the accuracy, with which we can design, compute and fabricate the patterns. These patterns can be binary, multilevel or continuous. Using an LCoS-based SLM instead of a static grating element enable us to have a programmable grating, whose grating period can be varied as desired. Spot array generations for multicast transmission scenarios in a reconfigurable VLC can be performed arbitrary.

The computer-generated phase grating element design typically involves an optimization procedure to minimize a fitness function that measures the similarity of the generated spot pattern with the targeted one. To date, the iterative Fourier-transform algorithms, such as gerchberg-saxton (GS) algorithm, have popularly used for fast optimization and most of them have well evaluated and documented [17]. GS algorithm was originally invented in the early of 1970s and has been widely used for various applications [18]. It is an iterative procedure which is simple and efficient for calculating the phase only. Although the algorithm can handle large amounts of data [19], it is very sensitive to initial parameters, i.e., random phase chosen and the desired amplitude distributions. Using GS algorithms, several iterations are normally required before convergence. In this research, an optimal procedure based on the conventional GS algorithm [17] was used to investigate the spot array generation at near-field for the direct implementation of a reconfigurable VLC system based on multisport configuration. Fig. 1 shows the flowchart of the optimal approach used in this research based on the iterative procedure of conventional GS algorithm. Similar as the conventional GS algorithm, in the initial iteration, a random phase $\phi_{in}(x, y)$ uniformly distributed in the range [0, 2π] is used. A function $f(x, y)$ is defined as

$$f(x, y) = A_{in}(x, y) \exp[i\phi_{in}(x, y)] \tag{1}$$

Where $A_{in}(x, y)$ is the targeted distribution of spot amplitude. A scaled Fourier transform of $f(x, y)$ is the field distribution of output F(u, v), which is expressed as

$$F(u, v) = FT\{f(x, y)\} = F_{\text{out}} \exp[i\phi_{\text{out}}(u, v)] \tag{2}$$

Since the targeted spot amplitude distribution in the Fourier plane is $A_{\text{out}}(u, v)$, the phase ϕ_{out} is left unchanged as it is derived from (2), but the amplitude $F_{\text{out}}(u, v)$ is replaced by the targeted

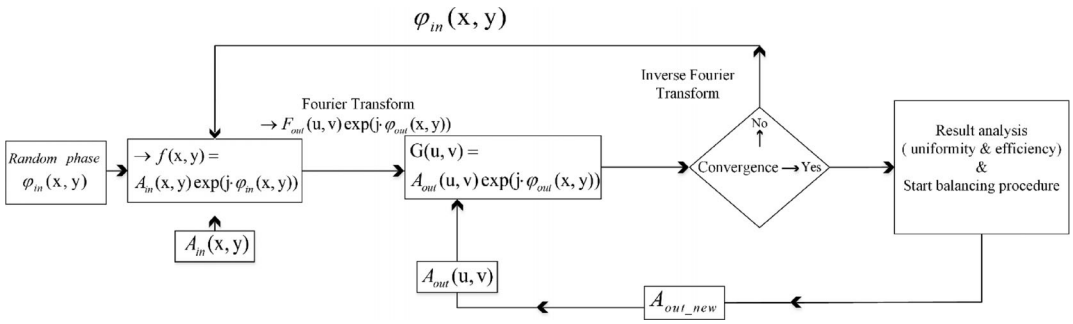

Fig. 1. Flow chart of the optimal procedure based on GS algorithm.

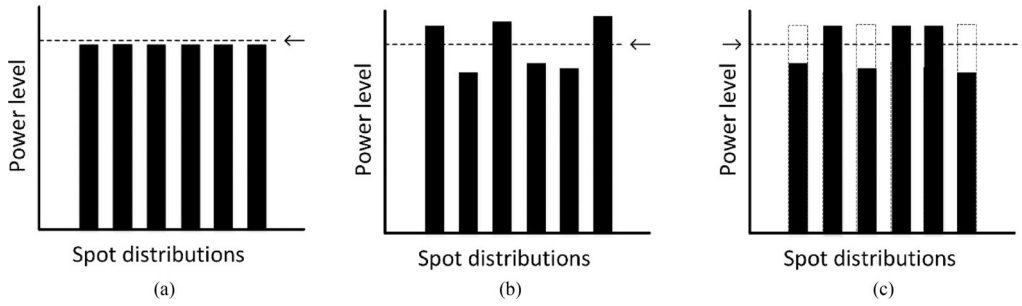

Fig. 2. Optimal design based on a balancing procedure. (a) Targeted. (b) After first convergence. (c) New targeted.

$A_{\text{out}}(u, v)$. Hence, a new function $G(u, v)$ is defined as

$$\mathrm{G}(u, v) = A_{\text{out}}(u, v)\exp[i\phi_{\text{out}}(u, v)] \tag{3}$$

An inverse Fourier transform is further conducted on $G(u, v)$ and for next iteration, the phase resulted from (3) is used as the input phase $\phi_{in}(x, y)$. After the first several iterations, it converges and tends to stagnate at local minima with high efficiency but worst uniformity. In the case of generating 1×6 spot array, it normally converges after five iterations. Here the efficiency E is defined as $\mathrm{E} = P_{\text{total}}/P_0$, where P_{total} is the power contained in all desired spots and P_0 is the total incident power. The spot power uniformity is defined as $\mathrm{U} = (P_{\max} - P_{\min})/(P_{\text{avg}})$, where $P_{\max}$ is the maximum spot power, $P_{\min}$ is the minimum spot power and P_{avg} is the average spot power of all desired spots. A lower spot power uniformity is desired for multispot configuration as each spot should have an equal power intensity in order to deliver the same data transmission rate. The quality of the algorithm's convergence is tested by obtaining the root mean square (RMS) value, which is defined as $\mathrm{RMS} = \sqrt{\sum_{i=1}^{n}(P_t - P_i)^2}$, where n is the spot number, P_t is the desired target spot power and P_i is the i_{th} spot power. The convergence process of the GS algorithm is very fast but characterized by the stagnation effect, which means that after a rapid decrease of the RMS in the course of several initial iterations, further iterations do not result in its significant decrease. The stagnation effect implies that the algorithm reaches a local minimum of the RMS. Although the stagnation at local minima limits the GS algorithm, with our approach, it can be optimized to achieve a good power uniformity of spot array while maintaining a high efficiency either in the near-field (Fresnel approximation) or in the far-field (Fraunhofer approximation) application. When the design of CGH is for near-field (Fresnel approximation) application, the quadratic phase factor, $\exp[j(k/2z)(\xi^2 + \eta^2)]$, [14] should be included in the (1) during the computing, otherwise it should be omitted.

The procedure used in our approach, is that the original (targeted) amplitude distribution $A_{in}(x, y)$ given as illustrated in Fig. 2(a) was applied into the initial iterative procedure of GS algorithm first.

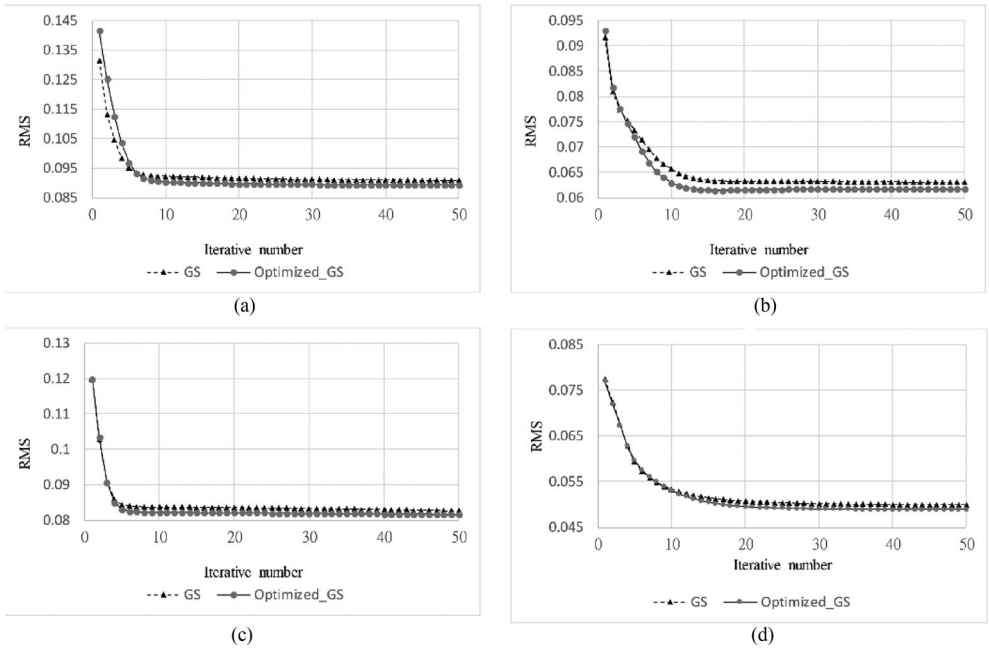

Fig. 3. RMS of spot array generation at 2.5 m. (a) RMS of 1 × 3_spot array. (b) RMS of 1 × 6_spot array. (c) RMS of 2 × 2_spot array. (d) RMS of 3 × 3_spot array.

The $A_{out}(u, v)$ obtained as illustrated in Fig. 2(b) from the subsequent convergence of GS initial iterative procedure was then used to define a new targeted amplitude distribution as illustrated in Fig. 2(c) for next round of GS iterative procedure. The definition of a new targeted amplitude distribution as illustrated in Fig. 2(c) was through a balancing procedure of amplitude distribution obtained from previous convergence result. In this balancing procedure, the average power level of amplitude distribution obtained from previous convergence result was setup as the power level of the new amplitude distribution for next round iterative procedure. The input phase used for next round iterative procedure with a new targeted amplitude distribution [Fig. 2(c)], is also the result (phase) obtained from the previous convergence rather than chosen randomly. Since the input phase from the previous convergence has leaded to a high light efficiency, after the reallocation of the power amplitude distribution, the spot power uniformity can be further improved through the following iteration procedures. In contrast to the original GS algorithm, the results with balancing procedure during the iterative procedure of GS algorithm was renamed as an optimized GS algorithm in this research.

Performance comparisons using holograms with 1920 × 1080 pixels (corresponding to the pixel number of the LCoS device used in the proposed experimental work) were simulated. From the simulation results in a variety of spot array generation scenarios, the RMS of GS and optimized GS algorithms has compared and a representative result (at a transmission distance of 2.5 m) is shown in Fig. 3. It is clear from Fig. 3 that after a rapid decrease of the RMS in the course of several initial iterations in both GS and optimized GS algorithms, further iterations do not result in its significant decrease. However, as illustrated in Fig. 4, in the case of generating 1 × 6 spot array as the representative result, we can see that spot power uniformity has been improved from 27% to 5%. Compared with the conventional GS algorithm, the proposed approach can rapidly reach a better spot power uniformity while maintaining the same high efficiency of conventional GS algorithm.

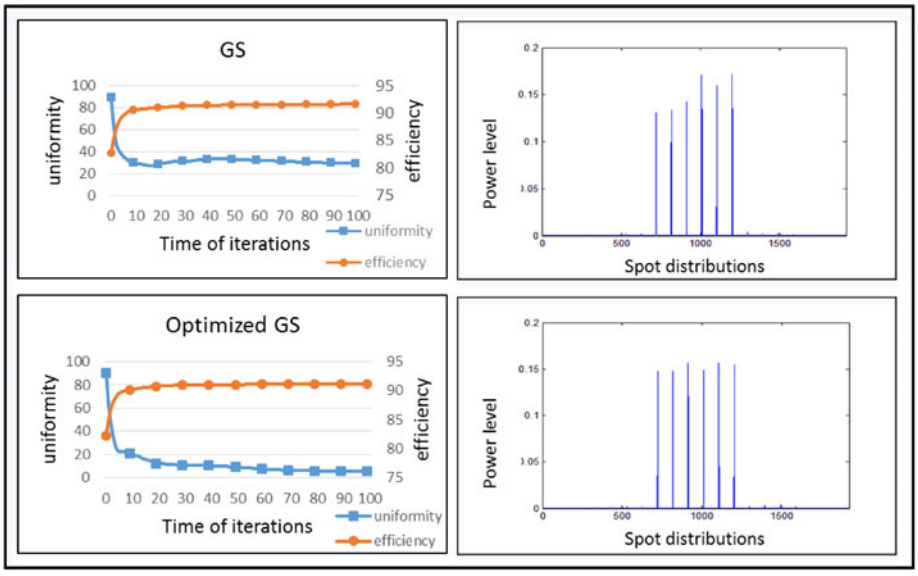

Fig. 4. Simulation results of GS & optimized GS algorithm.

3. Experimental Setup and Performance Evaluation

In this research, an experimental investigation of a VLC based on holographic spot array generation through an LCoS SLM for the direct implementation of a reconfigurable VLC system based on multisport configuration as illustrated in Fig. 5(a) is reported and for the proof of concept, an experimental setup as illustrated in Fig. 5(b) was implemented in order to evaluate the system performance. In this experimental research, a conventional blue LD (laser diode, PL 450B, OSRAM) was used as the light source of transmitter (TX). The blue LD has a single transverse mode and the central wavelength is 450 nm. The spectral linewidth of the LD is 0.67 nm and its maximum beam divergence at horizontal and vertical are 25 and 11 degree respectively.

In the digital transmission test, an arbitrary waveform generator (AWG, Keysight, 1GSa/s sampling rate) was used to store the signals for TX transmission. These stored signals were randomly generated and have modulated in advance through a computer program, Matlab from a PC (personal computer). Although several complex modulation schemes such as OFDM, and DMT have widely applied to maximize the transmission efficiency, they were all based on the employment of baseband modulation scheme such as M-ary Quadrature Amplitude Modulation (M-QAM). Therefore, M-QAM was used to explore the data transmission performance of the generated spot array in our research. Since the data encoding on the blue LD was based on the intensity modulation approach, the light emitted from the blue LD on TX was driven individually by modulated signals from AWG and biased separately by a DC current of 140 mA through a Bias Tees (Minicircuits, ZFBT-282-1.5A).

A collimating lens (L1) was first used to collimate the laser beams transmitted from TX and subsequently the polarization state of the collimated laser beams was adjusted to be paralleled with the director of the Liquid Crystal (LC) material by a polarizer before incident on the LCoS-based SLM in order to perform the phase modulation efficiently. The LCoS-based SLM device used was a phase only microdisplay (JD 9554, JDC, Taiwan) and all pixels on the device can be controlled through the upload of a hologram pattern that has designed.

The LCoS device was calibrated in the range [0, 2π] at the wavelength of 450 nm. Different near-field holograms (multilevel phase modulation) corresponding to different transmission distance were generated and used in our experiments to evaluate the system performance. This is different to the approach used in [20], where only one hologram (binary phase modulation) was used to compare the performance at different transmission distance. Moreover, the efficiency as well as spot power uniformity were also not reported in [20]. In our experiment, a lens after the SLM was not used as

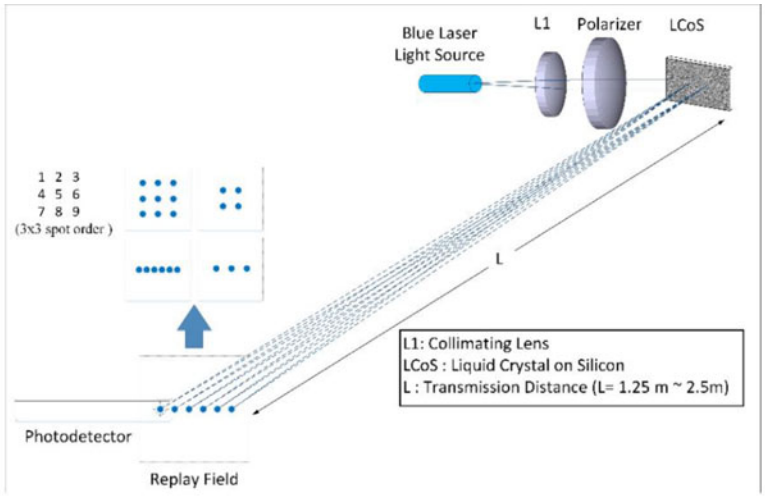

(a)

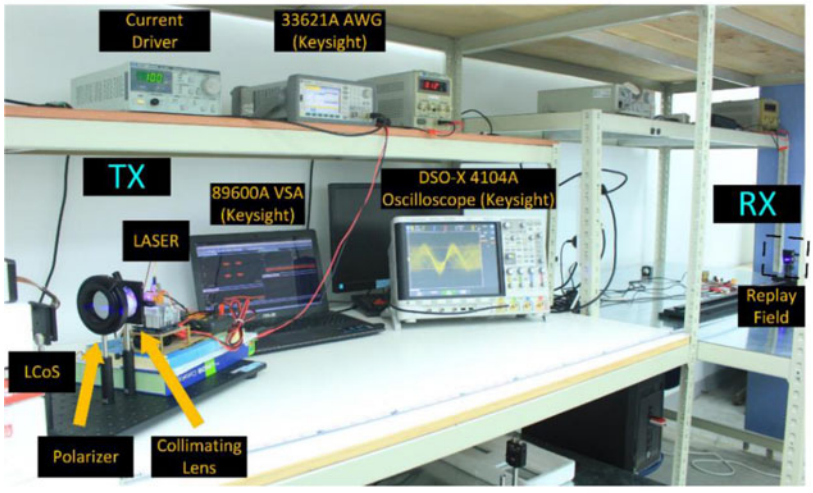

(b)

Fig. 5. Experimental performance evaluation. (a) System architecture based on LCoS SLM. (b) Setup of experimental system.

the design of the CGH patterns was based on Fresnel approximation (near-field). In the reply filed (receiver site), spot array generated from the LCoS device were measured directly by an amplified photodetector (EOT, ET-2030a) which has a conversion gain of 190 V/W for blue wavelength and has a diameter of 400 μm for active area. An amplifier with 11dB gain (Minicircuits) was used to amplify the received signals again before the signals were recorded by a real-time oscilloscope (Keysight, 5 GSa/s sampling rate). A vector signal analysis software (Keysight VSA89600) from a PC was then used to analyze the received signals from the oscilloscope directly.

4. Results and Discussions

Since the maximum data transmission rate of the system (each port) that can be used in the scenario of multiuser communication through spot array generation is limited by the lowest transmission rate of the port (spot). Therefore, the spot power uniformity and the efficiency in one dimension and two dimension spot array generations using the design of near-field CGH through GS and optimized GS algorithms at a transmission distance of 1.25 m$\sim$2.5 m have investigated and are compared as illustrated in Fig. 6(a) and (b) respectively. From the measurement results shown in Fig. 6, in

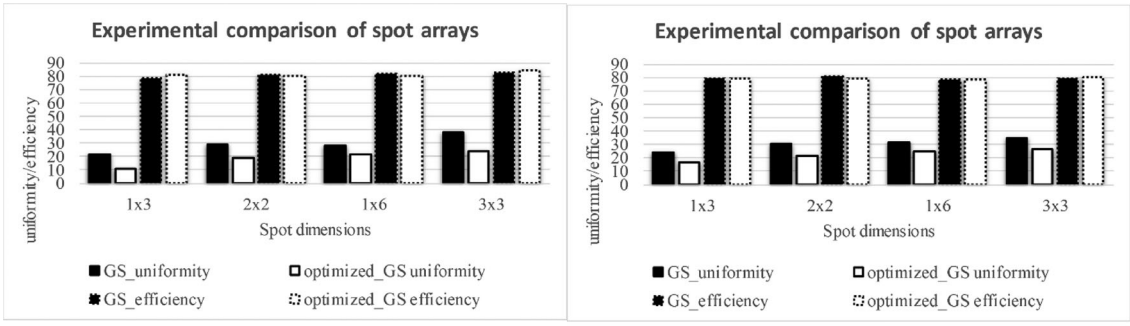

Fig. 6. Performance comparison of spot arrays. (a) 1.25 m. (b) 2.5 m.

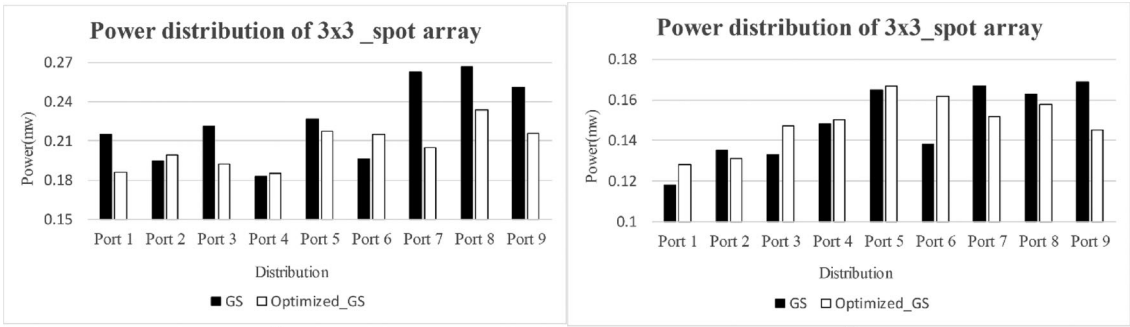

Fig. 7. Intensity distribution of 3×3 spot arrays. (a) 1.25 m. (b) 2.5 m.

the transmission distance of 1.25 m and 2.5 m, it is clear that the optimized GS algorithm can all maintain the same high efficiency as original GS algorithm but the spot power uniformity has all been significantly improved compared with original GS algorithm either in a one dimension or two dimension spot array generation scenarios. The intensity profiles of each spot were also measured using knife-edge method [21] and their power distributions using 3×3 spot arrays as the representative result at 1.25 m and 2.5 m are shown in Fig. 7(a) and (b) respectively. From the measurement results, it is obviously that the each spot generated based on the design of near-field CGH either through GS or optimized GS algorithms, all have different power intensity which means that for the same data transmission rate, each spot will not be able to achieve the same transmission quality i.e., Bit Error Rate (BER) due to the insufficient signal to noise ratio (SNR).

The transmission performance of multispot array generation based on near-field CGH design using baseband modulation scheme, 16-QAM at a transmission distance of 1.25 m$\sim$2.5 m was further experimentally evaluated. The measurement results are shown in Fig. 8(a) and (b) respectively. As illustrated in Fig. 8(a), when GS algorithm was used to generate two dimension spot array i.e., 3×3, at a transmission distance of 1.25 m, the maximum data transmission rate of each port measured was varied between 202 Mbps and 350Mbps (BER $= 10^{-3}$). Since spot array was generated based on the same modulated light source and for multispot configuration scenario, the maximum data rate of each spot should be the same and would be restricted by the port (spot) which has the lowest data transmission rate. Therefore the maximum data modulation speed of the system should be limited to 202 Mbps (port 4) in this case. However when an optimized GS algorithm was used, we can see that the port 4 which has the lowest data transmission rate of 202 Mbps has been raised to 240 Mbps. The improvement of the system's limitation is about 13.9%. Similar results have also measured when GS and optimized GS algorithm were used to generate two dimension spot array i.e., 3×3, at a transmission distance of 2.5 m. As compared from Fig. 8(b), we can observe that the maximum data modulation speed of the system (BER $= 10^{-3}$) will be restricted by the port

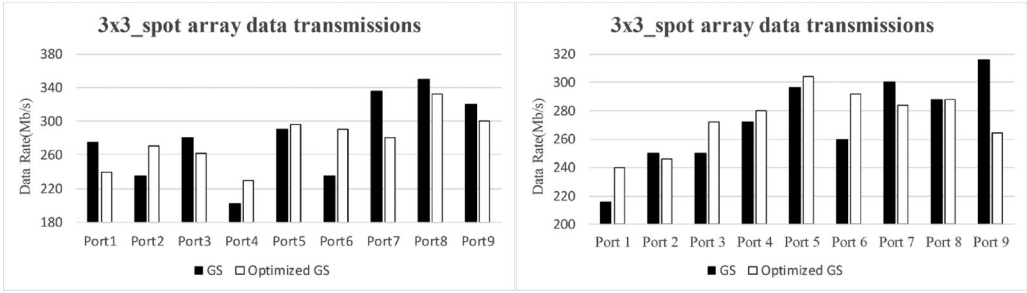

Fig. 8. Data transmission performance of each spot (16-QAM, BER $= 10^{-3}$). (a) 1.25 m. (b) 2.5 m.

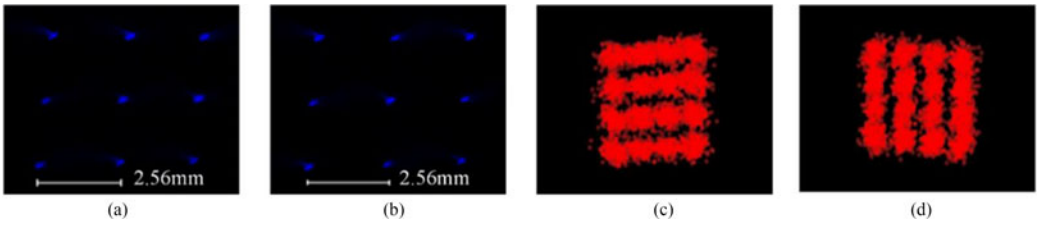

Fig. 9. Comparisons of data transmission performance at 1.25 m (3×3 spot array, 16-QAM). (a) 3×3 spot profiles (GS). (b) 3×3 spot profiles (Optimized GS). (c) Constellation diagram (GS, port 4). (d) Constellation diagram (Optimized GS, port 4).

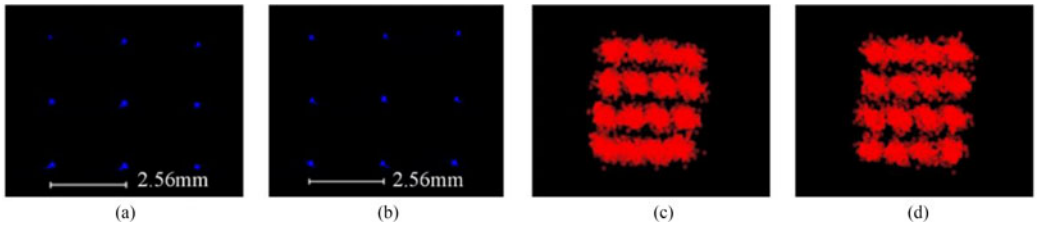

Fig. 10. Comparisons of data transmission performance at 2.5 m (3×3 spot array, 16-QAM). (a) 3×3 spot profiles (GS). (b) 3×3 spot profiles (Optimized GS). (c) Constellation diagram (GS, port 1). (d) Constellation diagram (Optimized GS, port 1).

1 which is about 216 Mbps and after the use of an optimized GS algorithm, the port 1 which has the lowest data transmission rate of 216 Mbps has been raised to 240 Mbps. The improvement of the system's limitation is about 11.1%. From these measurement results comparing the received power intensity and the corresponding data rate (BER $= 10^{-3}$) of each port as illustrated in Figs. 7 and 8 respectively, we can conclude that the port which has received a higher power, can normally achieve a higher data transmission rate under the same evaluation criterion (BER $= 10^{-3}$).

The spot profiles using 3×3 spot array as the representative result generated from GS and optimized GS algorithm at a transmission distance of 1.25 m are shown in Fig. 9(a) and (b) respectively. Their constellation diagrams of the spot (port 4) which has the lowest data rate of 202 Mbps and 240 Mbps are shown in Fig. 9(c) and (d) respectively. The spot profiles using 3×3 spot array as the representative result generated from GS and optimized GS algorithm at a transmission distance of 2.5 m are also shown in Fig. 10(a) and (b) respectively. Their constellation diagrams of the spot (port 1) which has the lowest data rate of 216 Mbps and 240 Mbps are shown in Fig. 10(c) and (d) respectively. The BERs of all the measured constellation diagrams shown in Figs. 9 and 10 were all estimated to be less than 10^{-3} which meets the FEC (Forward Error Correction) limitations (BER $\leq 3.8 \times 10^{-3}$) [22]. Although the maximum data transmission rate of each spot that can be transmitted in our proposed system, is limited by the lowest transmission rate of the port (spot) i.e., 240 Mbps (BER $= 10^{-3}$) in a 3×3 spot array generations, a system capacity over 2 Gbps

(9×240 Mbps) can be achieved in the configuration of 3×3 spot array generations. A higher system capacity is also possible when the numbers of the spot are increased.

5. Conclusion

In this paper, we have presented and experimentally demonstrated a reconfigurable VLC system based on holographic spot array generation for multisport configuration. To the best of our knowledge, this is the first time that multisport configuration based on holographic spot array generation approach for an alternative implementation of a VLC system has experimentally demonstrated. An optimal design of near-field CGHs based on GS iterative algorithm for intensity-weighted spot array generation was experimentally implemented through LCoS-based SLM. The system performance was evaluated in terms of spot array uniformity and data transmission performance at a transmission distance of 1.25 m$\sim$2.5 m and the results shown that a significant improvement over 11% has been achieved either in a one-dimension or two-dimension spot array generation scenarios. The works presented in this paper will provide an efficient approach for the direct implementation of a reconfigurable VLC system based on multisport configuration.

References

[1] D. Nesset, "NG-PON2 technology and standards," *J. Lightw. Technol.*, vol. 33, no. 5, pp. 1136–1143, 2015.
[2] M. A. Khalighi and M. Uysal, "Survey on free space optical communication: A communication theory perspective," *IEEE Commun. Surveys Tuts.*, vol. 16, no. 4, pp. 2231–2258, Oct.–Dec. 2014.
[3] J. M. Kahn and J. R. Barry, "Wireless infrared communications," *Proc. IEEE*, vol. 85, no. 2, pp. 265–298, Feb. 1997.
[4] F. E. Alsaadi and J. M. H. Elmirghani, "Performance evaluation of 2.5 Gbit/s and 5 Gbit/s optical wireless systems employing a two dimensional adaptive beam clustering method and imaging diversity detection," *IEEE J. Sel. Areas Commun.*, vol. 27, no. 8, pp. 1507–1519, Oct. 2009.
[5] A. G. Al-Ghamdi and J. M. H. Elmirghani, "Spot diffusing technique and angle diversity performance for high speed indoor diffuse infra-red wireless transmission," *IEE Proc.—Optoelectron.*, vol. 151, no. 1, pp. 46–52, 2004.
[6] H. Le Minh *et al.*, "A 1.25-Gb/s indoor cellular optical wireless communications demonstrator," *IEEE Photon. Technol. Lett.*, vol. 22, no. 21, pp. 1598–1600, Nov. 2010.
[7] K. Wang, A. Nirmalathas, C. Lim, and E. Skafidas, "4 $\times$ 12.5 Gb/s WDM optical wireless communication system for indoor applications," *J. Lightw. Technol.*, vol. 29, no. 13, pp. 1988–1996, 2011.
[8] F. Feng, I. H. White, and T. D. Wilkinson, "Free space communications with beam steering a two-electrode tapered laser diode using liquid-crystal SLM," *J. Lightw. Technol.*, vol. 31, no. 12, pp. 2001–2007, 2013.
[9] S. T. Jovkova and M. Kavehard, "Multispot diffusing configuration for wireless infrared access," *IEEE Trans. Commun.*, vol. 48, no. 6, pp. 970–978, Jun. 2000.
[10] A. T. Hussein, M. T. Alresheedi, and J. M. H. Elmirghani, "20 Gb/s mobile indoor visible light communication system employing beam steering and computer generated holograms," *J. Lightw. Technol.*, vol. 33, no. 24, pp. 5242–5260, 2015.
[11] M. T. Alresheedi and J. M. H. Elmirghani, "High-Speed indoor optical wireless links employing fast angle and power adaptive computer-generated holograms with imaging receivers," *IEEE Trans. Commun.*, vol. 64, no. 4, pp. 1699–1710, Apr. 2016.
[12] C. Lee *et al.*, "4 Gbps direct modulation of 450 nm GaN laser for high-speed visible light communication," *Opt. Exp.*, vol. 23, pp. 16232–16237, 2015.
[13] Y.-C. Chi, D.-H. Hsieh, C.-T. Tsai, H.-Y. Chen, H.-C. Kuo, and G.-R. Lin, "450-nm GaN laser diode enables high-speed visible light communication with 9-Gbps QAM-OFDM," *Opt. Exp.*, vol. 23, pp. 13051–13059, 2015.
[14] J. W. Goodman, *Introduction to Fourier Optics*. San Francisco, CA, USA: Freeman, 2004.
[15] F. B. McCormick, "Free-space interconnection techniques," in *Photonics in Switching*, J. E. Midwinter, Ed. New York, NY, USA: Academic, 1993.
[16] N. Streibl, "Beam shaping with optical array generators," *J. Modern Opt.*, vol. 36, no. 12, pp. 1559–1573, 1989.
[17] F. Wyrowski and O. Bryngdahl, "Iterative Fourier-transform algorithm applied to computer holography," *J. Opt. Soc. Amer. A*, vol. 5, no. 7, pp. 1058–1065, 1988.
[18] A. Rundquist, A. Efimov, and D. Reitze, "Pulse shaping with the Gerchberg-Saxton algorithm," *J. Opt. Soc. Amer. B*, vol. 19, no. 10, pp. 2468–2478, 2002.
[19] G. Zhou, X. Yuan, P. Dowd, Y. Lam, and Y. Chan, "Design of diffractive phase elements for beam shaping: Hybrid approach," *J. Opt. Soc. Amer. A*, vol. 18, no. 4, pp. 791–800, 2001.
[20] P. García-Martínez, M. M. Sánchez-López, J. A. Davis, D. M. Cottrell, D. Sand, and I. Moreno, "Generation of bessel beam arrays through dammann gratings," *Appl. Opt.*, vol. 51, no. 9, pp. 1375–1381, 2012.
[21] D. Wright, P. Greve, J. Fleischer, and L. Austin, "Laser beam width, divergence and beam propagation factor -and international standardization approach," *Opt. Quantum Electron.*, vol. 24, pp. S993–S1000, 1992.
[22] J. Vucic *et al.*, "230 Mbit/s via a wireless visible-light link based on OOK modulation of phosphorescent white LEDs," in *Proc. Opt. Fiber Commun. Conf., OSA Tech. Digest Opt. Soc. Amer.*, 2010, Paper OThH3.